

## ORIGINAL ARTICLE

# Measuring Symmetry in Children With Cleft Lip. Part 3: Quantifying Nasal Symmetry and Nasal Normalcy Before and After Unilateral Cleft Lip Repair

Shu Liang, B.Sc., Linda Shapiro, Ph.D., Raymond Tse, M.D.

**Objective:** The purpose of this project was to develop objective computer-based methods to measure nasal asymmetry and abnormality in children undergoing treatment of unilateral cleft lip (UCL) and to determine the correlation of these measures to clinical expectations.

**Participants:** Thirty infants with UCL undergoing cleft lip repair; 27 children with UCL aged 8 to 10 years who had previously undergone cleft lip repair; 3 control infants; 3 control children aged 8 to 10 years.

**Interventions:** To measure nasal symmetry, we used a process of depth mapping and calculated the Depth Area Difference. To measure abnormality, we used the reconstruction error from Principle Component Analysis (PCA) that was based upon characteristics of a dataset of over 2000 images of normal control subjects.

**Main Outcome Measures:** Depth Area Difference and PCA Reconstruction Error for cleft type, changes with surgery, and individual subjects ranked according to cleft severity were assessed.

**Results:** Significant differences in Depth Area Difference and PCA Reconstruction Error were found between cleft types and found before and after surgery. Nasal symmetry and normalcy scores for infants with UCL approached those of controls after surgery, and there was a strong correlation with ranked cleft severity. For older children, measures of nasal symmetry and abnormality were better than infants prior to repair but worse than infants following UCL repair.

**Conclusions:** Our computer-based 3D analysis of nasal symmetry and normalcy correlated with clinical expectations. Automated processing made measurement convenient. Use of these measures may help to objectively measure cleft severity and treatment outcome.

KEY WORDS: *cleft lip; unilateral cleft lip; normality; PCA reconstruction; symmetry; 3D stereophotogrammetry; anthropometry; infant*

Cleft lip occurs in approximately 1 in 940 newborns (Parker et al., 2010) and results in a complex three-dimensional (3D) facial deformity of the lip, nose, and midface. Treatment occurs over multiple stages and involves multiple specialties. The relative merit of different techniques, procedures, and protocols is difficult to determine due to the lack of valid, objective, and convenient outcome measures. This is the third study in a series that examines different ways of measuring symmetry as an

indication of cleft severity and treatment success (Wu et al., 2015, 2016). The goal of all of these projects is to develop and validate automated computer-based measures that cleft team providers can use to evaluate the effects of treatments on large numbers of patients, easily and conveniently. These measurements would ultimately provide a means for evidence-based care and improvements in outcome

In our first study, we developed and evaluated various computer-based methods of defining the 3D midfacial reference plane (Wu et al., 2015). By ignoring the nasolabial region, this plane would allow consistent measurements for the same subject through treatment and between subjects. In our second study, we developed and evaluated different ways of quantifying 3D nasolabial symmetry (Wu et al., 2016). We found that measurements that considered all the available surface data in a given region performed better than those that were based on individual landmarks. We also found that all of the measures could differentiate subjects according to preoperative severity and could detect changes following surgery. Given that residual nasal deformity is the most common and stigmatizing feature following cleft lip repair, we wanted to develop more specific ways to quantify abnormalities of the nose.

---

Shu Liang is graduate student, Department of Computer Science and Engineering, University of Washington; Dr. Shapiro is Professor, Department of Computer Science and Engineering, University of Washington; Dr. Tse is Attending Surgeon, Division of Craniofacial and Plastic Surgery, Department of Surgery, Seattle Children's Hospital, University of Washington, Seattle, Washington.

Funding Sources: Seattle Children's Hospital CCTR TRIPP Fund, Seattle Children's Hospital CCTR Pediatric Pilot Fund (NIH U01DE20050).

Financial disclosures: None.

Conflicts of interest: None.

Submitted February 2016; Revised April 2016; Accepted April 2016.

Address correspondence to: Dr. Raymond Tse, Seattle Children's Hospital, 4800 Sand Point Way NE, M/S OB.9.527, Seattle, WA 98105. E-mail: raymond.tse@seattlechildrens.org.

DOI: 10.1597/16-035

**TABLE 1 Characteristics of Patients Whose Images Were Used in This Study**

	<i>UCL Infant (n = 30)</i>	<i>UCL 8–10 y (n = 28)</i>	<i>Control Infant (n = 3)</i>	<i>Control 8–10 y (n = 3)</i>
Mean age at photo	5.8 mo	10.6 y	6.2 mo	10.1 y
Male:Female	17:13	17:10	1:2	1:2
Laterality of cleft (Left:Right)	17:13	17:10	N/A	N/A
Syndrome	2*	2**	N/A	N/A
Cleft extent				
Cleft lip	14	2	N/A	N/A
Cleft lip and alveolous	3	3	N/A	N/A
Cleft lip and palate	13	22	N/A	N/A
Cleft lip type				
Microform	0	1	N/A	N/A
Incomplete	14	2	N/A	N/A
Complete + Soft Tissue Band***	7	0	N/A	N/A
Complete	9	12	N/A	N/A
Unknown	0	12	N/A	N/A

\* Popliteal pterygium and chromosomal abnormality NYD.

\*\* van der Woude and Pierre Robin.

\*\*\* Differentiated from incomplete cleft lip by presence of a complete cleft alveolous.

The purpose of this research was to develop measures of nasal asymmetry and nasal “normalcy” with unilateral cleft lip (UCL) and to determine if these correlated with clinical expectations.

## METHODS

This study was reviewed and approved by our institutional review board. Consent was obtained from all subjects to participate in this project.

### Clinical Sample Set

We examined the 3D images of 30 infants with UCL immediately before (UCL Infant Prerepair) and after (UCL Infant Postrepair) primary cleft lip repair; 28 children aged 8 to 10 years who had previously undergone cleft lip repair (UCL 8 to 10 years Postrepair); 3 control infant subjects (Control Infant) with no craniofacial differences; and 3 control children aged 8 to 10 years (Control 8 to 10 years) with no craniofacial differences. Demographics and cleft type are summarized in Table 1.

### Infants With UCL

Children with UCL at our center undergo cleft lip repair at 6 months of age. Consecutive families of infants with UCL who presented to the senior author in the Craniofacial Clinic were recruited. Components of their primary cleft lip repair included markings according to the Fisher technique (Fisher, 2005; Tse and Lien, 2015), primary septoplasty, reconstruction of lateral nasal wall and nasal floor, and reconstruction of orbicularis oris (Tse, 2013). Matching pre- and postoperative images of the same subject were used in this study (UCL Infant Prerepair and UCL Infant Postrepair respectively). Images were captured in clinic at the preoperative and immediate postoperative visits.

### Children 8 to 10 Years With Prior UCL Repair

Consecutive patients aged 8 to 10 presenting to any provider in the Craniofacial Clinic were recruited. These patients underwent varying courses of treatment. Of the 28 subjects, primary cleft lip repair was performed at our institution for 16 and at another institution for 12. Ten underwent secondary cleft lip revision. All 22 patients with cleft palate underwent cleft palate repair, and 21 patients underwent alveolar bone grafting. Nine patients underwent secondary tip rhinoplasty, and 4 underwent septorhinoplasty.

Only a single image was analyzed for each of these subjects, as preoperative 3D images were not available.

### 3D Images and Processing

3D facial images were captured by our center’s professional imaging technologist using the 3dMDvultus cranial system (3dMD LLC, Atlanta, GA).

All 3D meshes were precleaned (face recognized and all other body parts and objects removed) and aligned to a standard frontal pose using a previously described automated method (Wu et al., 2014).

### Nasal Symmetry: Depth Area Difference

We used a method we call “Depth Area Difference” to measure how different the two sides of the nose are relative to a midfacial reference plane.

With each facial mesh pose normalized to the standard frontal pose, the 3D image was rendered as a frontal 2D image. Eighty-three facial landmarks were detected using the shareware Face++ (Megvii Inc., Beijing City, China). Face++ is a state-of-the-art vision service that provides a software development kit for face recognition and facial landmark detection. We chose to use it given that it seemed more reliable and accurate in

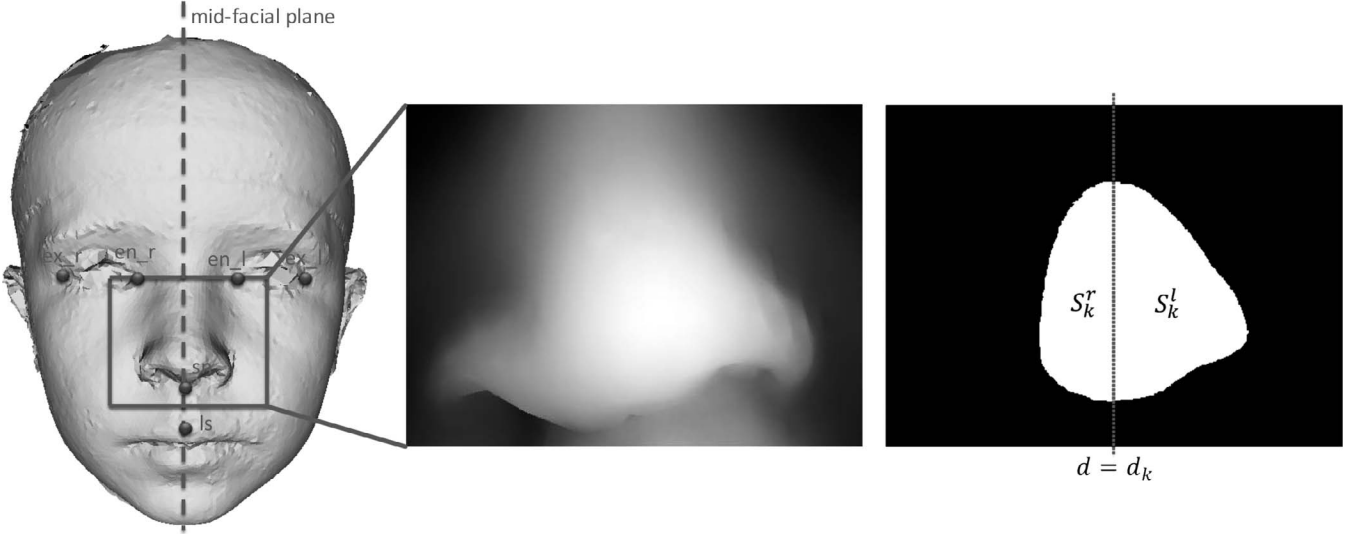


**FIGURE 1** Image analysis. Left: Example of 3D facial mesh of a subject without cleft lip; following automated cropping, pose-normalization, and placement of the mid-facial plane, the nasolabial region was isolated. Center: Example of depth map of the nasolabial region for a subject with unilateral cleft lip; each pixel was assigned a depth value; pixel depth in this image is represented on the scale from white to black. Right: An example of a given cutting plane ( $d^k$ ) for a subject with unilateral cleft lip. The difference in surface area across the midfacial plane (left surface area,  $S_k^r$  vs right surface area,  $S_k^l$ ) can be calculated at each depth,  $k$ , to yield an index of symmetry (Depth Area Difference).

identifying facial landmarks. The 83 2D landmarks were transferred to the 3D space, and the geometric midline of the eye and mouth points was used to compute the midfacial reference plane. The 3D mesh was then rotated and translated so that its midfacial reference plane was aligned with the  $x = 0$  plane.

We focused on the nose region  $R_{nose}$  of each mesh as defined in Figure 1:

$$R_{nose} = \{(x, y, z) \mid |x| \leq x_{boundary}, y_{min} \leq y \leq y_{max}\}$$

The horizontal boundary  $x_{boundary}$  was defined using the four eye corner points, endocanthions ( $en_l$  and  $en_r$ ) and exocanthions ( $ex_l$  and  $ex_r$ ):

$$x_{boundary} = \max(0.75x_{en_l} + 0.25x_{ex_l}, -0.75x_{en_r} - 0.25x_{ex_r})$$

The vertical boundaries  $y_{min}$  and  $y_{max}$  were defined using the four eye corner points and two nose points, subnasale ( $sn$ ) and labiale superius ( $ls$ ):

$$y_{max} = (y_{en_r} + y_{en_l})/2$$

$$y_{min} = 0.75y_{sn} + 0.25y_{ls}$$

The nose region was cropped from each 3D mesh (Fig. 1), and the gray-scale depth image—in which each pixel value was the  $z$ -value of a 3D point on the head mesh—was constructed for the nose portion. The head was centered so that the midfacial plane was aligned with the midline of the depth image. The depth value for each pixel was rescaled so that the point with the maximum  $z$ -value (usually the nose tip) had a pixel value of 255 and the point with the minimum  $z$ -value

was 0. The length and width of all depth images were then normalized to an equal scale of  $436 \times 344$  (Fig. 1).

Given a set of depth thresholds ( $d_1, \dots, d_k, \dots, d_x$ ), the depth image was cut by several coronal cutting planes. On each cutting plane with depth value  $d$ , the 2D points with pixel values larger than  $d$  were kept, forming a continuous area (Fig. 1). On the  $k$ -th cutting plane, we defined the area on the left side of the mid-facial plane as  $S_k^l$  and the area on the right side as  $S_k^r$ . Since the cleft region could be on either side, we defined the Depth Area Difference using absolute values.

$$Area\_diff = \sum_{k=1}^X |S_k^l - S_k^r|$$

In our experiments, we set  $d_k = (25 + k) / 40 \times 255$ ,  $X = 14$ , which means that  $d_k$  was from 165.75 to 255.

Figure 2 shows an example of nose region silhouettes of a given depth level. The left case illustrates an infant before cleft lip repair in which the nose is deformed and the nasal tip is deviated from the facial midline. The case in the middle shows the postsurgery result for the same subject, in which the nose is corrected to the center, but the alar shapes on two nose sides are still different. The right case is the silhouette of a normal control subject's nose, which is more symmetric with a smaller Depth Area Difference.

### **Nasal Normalcy: Principle Component Analysis Reconstruction Error**

To assess how different a given nose is from a “normal nose,” we used a method known as Principle

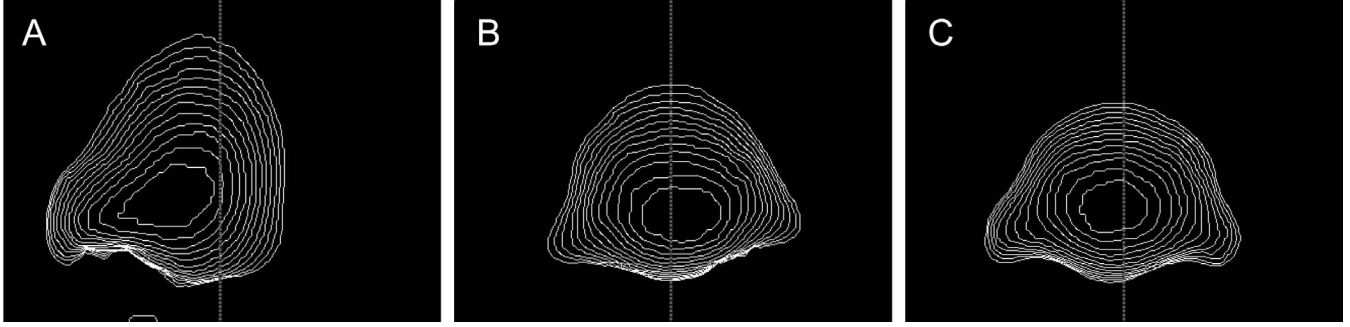


**FIGURE 2** Example of silhouettes of nasolabial depth areas for different infant noses. **A:** Subject with unrepaired cleft lip. **B:** The same subject immediately following cleft lip repair. **C:** Age-matched control subject with “normal” nose.

Component Analysis to construct a “normal” reference and measured the reconstruction error. First, Principle Component Analysis (PCA) was applied to the 3D mesh images of a large set of normal control subject noses to construct a set of “basis vectors” that forms a space capable of representing any nose shape. We hypothesized that a normal nose could be reconstructed as a linear combination of basis vectors with a low reconstruction error, whereas the noses of children with cleft lip would yield large reconstruction errors. The reconstruction error could then be used as an indicator of how different a nose was from “normal.”

We used the 3D facial meshes of 2279 normal Caucasian individuals with no craniofacial differences, aged 3 to 40 (3D Facial Norms Database<sup>1</sup>) for PCA training. All subjects were face forward with a neutral expression. These 3D meshes had been precleaned and aligned by experts for research purposes.

The nose region of each head was represented by a depth image matrix of  $436 \times 344$  dimensions. Each image matrix was converted into a depth vector as follows:

$$T = (I_1, I_2, I_3, \dots, I_M)$$

where  $M = 436 \times 344$ , and  $I$  was the pixel value in the depth image.

A normal nose model was constructed using the 3D Facial Norms Database with each nose represented by its depth vector  $T_i$ . Since all the depth images are scaled to the same size, a new nose shape  $T_{new}$  could be expressed by a linear combination of the depth vectors of the  $N$  exemplar normal noses:

$$T_{new} = \sum_{i=1}^N \alpha_i T_i = \bar{T} + \sum_{i=1}^N \alpha_i (T_i - \bar{T})$$

$$\sum_{i=1}^N \alpha_i = 1$$

where  $T$  is the average depth vector, and  $\alpha_i$  are coefficients.

Principle Component Analysis (PCA; Sirovich and Kirby, 1987; Jolliffe, 2012) is a common method used to compress data, in which  $N$ -dimensional data is projected into an  $n$ -dimensional space, while preserving most of the information of the data set. A set of orthogonal basis vectors is constructed from the eigenvectors  $E_i$  of the covariance matrix of the depth vectors. A new nose shape can be approximated from only  $n$  eigenvectors by:

$$T'_{new} = \bar{T} + \sum_{i=1}^n \beta_i E_i$$

where  $\beta_i$ 's are coefficient,  $E_i$  is in descending order of the eigenvalues. In our experiment, we chose  $n = 100$ , taking the top 100 eigenvectors as our normal nose basis.

A new nose shape vector could be projected to the normal nose space and its coefficient vector  $\vec{\beta}$  obtained by minimizing the least-squares distance between the best approximation and the input shape  $T_{new}$ :

$$S_{error} = \min_{\vec{\beta}} \left\| \left( \bar{T} + \sum_{i=1}^n \beta_i t_i \right) - T_{new} \right\|_2^2$$

The result  $S_{error}$  was the score for our PCA reconstruction error measurement. A very deformed cleft nose region would have a large reconstruction error because the principal components of the normal noses cannot fit the deformed nose well.

Figure 3 shows the error maps for two cleft noses after PCA reconstruction in which the top subject's nose is more severely deformed than the bottom subject's nose. A bright yellow region can be observed on the alar regions of the top head, indicating a larger distance to normal noses.

<sup>1</sup> Morphometric data from normal faces were obtained from FaceBase ([www.facebase.org/facial\\_norms/](http://www.facebase.org/facial_norms/)) and were generated by project VOIDEO2008. The FaceBase Data Management Hub (voideo20057) and the FaceBase Consortium are funded by the National Institute of Dental and Craniofacial Research.

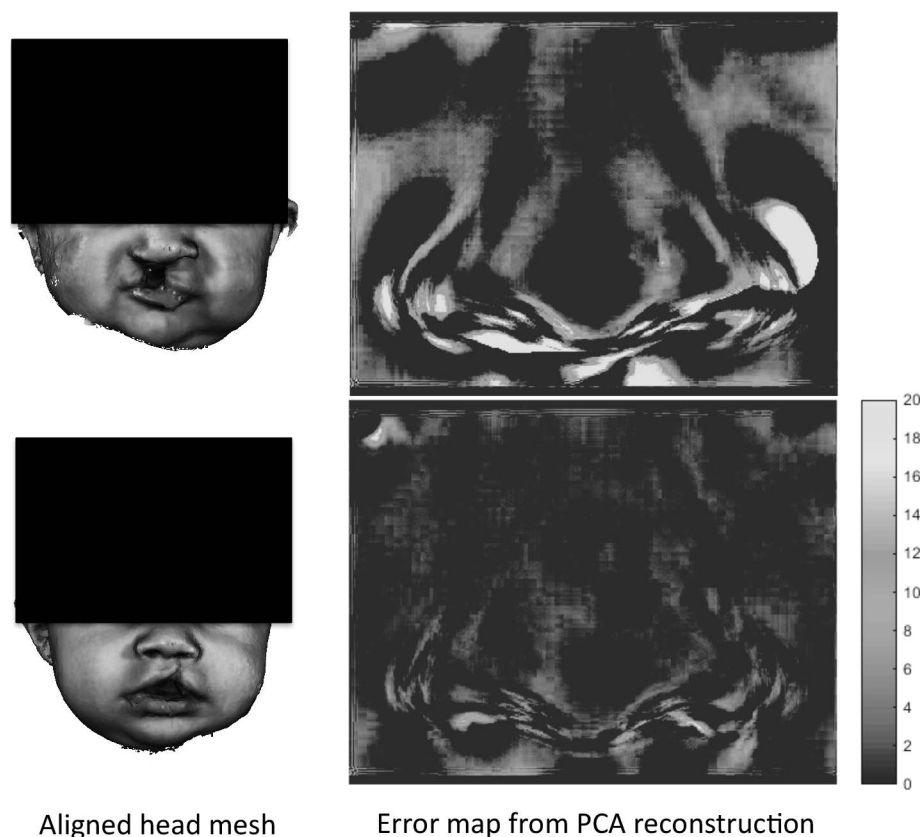


**FIGURE 3** PCA reconstruction. Left: The 3D facial meshes of two subjects with different severities of unilateral cleft lip nasal deformity are displayed. Right: The corresponding error maps are displayed. More yellow indicates greater reconstruction error, and this was used as an index of how much a given nose deviated from that of normal controls.

### *Rank Order of Cleft Severity*

We have previously found that expert cleft surgeons can reliably rank infants in the order of preoperative cleft severity (Fisher et al., 2008). Infant subjects with UCL were ranked in order of decreasing cleft lip nasal deformity. We created a digital “sorting board” in which mesh images could be sorted. Each mesh image was enlarged and rotated synchronously with the adjacent ordered images so the 3D form could be examined and compared by the blinded cleft surgeon (RT). This rank order was considered the ground truth for preoperative severity.

### *Statistical Analysis*

Mean Depth Area Difference and PCA Reconstruction Errors for subjects with the various types of cleft lip were evaluated using *t* test. A *P*-value of  $<.05$  was considered significant.

The correlation of measures of nasal symmetry and normalcy (Depth Area Difference and Principle Component Analysis respectively) were compared to the expert surgeon rank order of preoperative cleft severity

for infants with UCL using Pearson’s correlation coefficient.

## RESULTS

### *Nasal Symmetry: Depth Area Differences Before and After Primary Cleft Lip Repair*

Infants with cleft lip had a mean Depth Area Difference of  $10.0 \pm 5.61 \times 10^4$  before surgery, and it decreased to  $3.07 \pm 2.20 \times 10^4$  following cleft lip repair. For control infants, the Depth Area Difference was similar to that of infants with cleft lip repair after surgery but was even smaller, with a mean of  $2.59 \pm 0.44 \times 10^4$ .

The older children who had previously undergone cleft lip repair (UCL 8 to 10 year Postrepair group) were completely different individuals. Their average Depth Area Difference ( $5.13 \pm 3.59 \times 10^4$ ) was 72% greater than that of Control 8 to 10 year group ( $1.43 \pm 0.10 \times 10^4$ ). Compared to the infants following surgery (UCL Infant Postrepair group), the average Depth Area Difference for the older group (UCL 8 to 10 year Postrepair group) was 40% greater ( $5.13$  versus  $3.07 \times 10^4$ ).

We found that the Depth Area Difference for the older control group was 45% less than that for the Infant Control group ( $1.43$  versus  $2.59 \times 10^4$ ).

### ***Nasal Normalcy: PCA Reconstruction Errors Before and After Primary Cleft Lip Repair***

Infants with cleft lip had a mean PCA Reconstruction Error of  $38.41 \pm 29.43$  before surgery, and it decreased to  $13.42 \pm 8.14$  (change of 65.1%) following cleft lip repair. For control infants, the PCA Reconstruction Error was similar to that of infants with cleft lip repair after surgery but was even smaller, with a mean of  $9.40 \pm 2.80$ .

The average PCA reconstruction error ( $18.14 \pm 5.62$ ) for the older children (UCL 8 to 10 year Postrepair group) was 81% greater than that of Control 8 to 10 year group ( $3.41 \pm 1.11$ ). Compared to the infants following surgery (UCL Infant Postrepair group), the average PCA Reconstruction Error for the older group (UCL 8 to 10 year Postrepair group) was 26% greater ( $18.14$  versus  $13.42$ ).

We found that the PCA Reconstruction Error for the older control group was 64% less than that for the Infant Control group ( $3.41$  versus  $9.40$ ).

### ***Comparison of Groups Based on Cleft Type***

The Depth Area Difference measurement could differentiate infant subjects according to cleft type prior to cleft lip repair. Mean values for subjects with complete UCL, complete with band, and incomplete UCL were  $14.1 \times 10^4$ ,  $11.4 \times 10^4$ , and  $6.7 \times 10^4$ . The mean value for normal infant controls was  $2.59 \times 10^4$ . There was a statistically significant difference in mean Depth Area Difference for each of the four groups compared to each other, except for between UCL complete versus UCL complete with band and between UCL complete with band versus UCL incomplete.

After cleft lip repair, the mean Depth Area Difference measures for subjects with complete, complete with band, and incomplete UCL were  $2.8 \times 10^4$ ,  $3.0 \times 10^4$ , and  $3.3 \times 10^4$ . All these values were similar to each other and to that of infant controls ( $2.59 \times 10^4$ ).

The PCA Reconstruction Error measurement could also differentiate infant subjects according to cleft type prior to cleft lip repair. Mean values for subjects with complete, complete with band, and incomplete UCL were 75, 34, and 17. The mean value for normal infant controls was 9. There was a statistically significant difference in mean PCA Reconstruction Error for each of the four groups compared to each other, except for between UCL complete versus UCL complete with band ( $P = .08$ ).

After cleft lip repair, the mean PCA Reconstruction Error measures for subjects with complete, complete

with band, and incomplete UCL were 18, 14, and 10. These values were similar; however, a statistically significant difference remained between UCL complete versus UCL incomplete. Postoperative values for each group were also similar to that of infant controls (9) except for the UCL complete group, where a statistically significant difference remained.

### ***Correlation to Ranking of Infants With UCL***

For the Depth Area Difference, there was a good correlation (0.70) with expert ranking. Following surgical repair, the correlation coefficient dropped to 0.13, which is consistent with the expected correction of the presurgical asymmetry. For the PCA Reconstruction Error, the correlation coefficient was 0.66, and reduced to 0.14 after cleft lip repairs, which is again consistent with normalization of nasal shape following surgery, independent of the initial deformity. The correlation coefficients between the ranking and the score improvements were 0.58 and 0.69, which suggested that larger improvements were achieved in the more severe cases.

The distribution of the two measurement scores is shown in Figures 4 and 5. A trend that measures of nasal symmetry and normalcy before surgery converge with the same measures after surgery and approximate those of age-matched controls can be seen.

## **DISCUSSION**

3D stereo photogrammetry provides a convenient way to capture 3D facial form and allows for further objective analysis. Current systems use multiple digital cameras that produce a mesh representation of the surface shape with a corresponding texture representation of color values. The rapid capture (<2 msec) has allowed 3D stereo photogrammetry to be used on infants and children with cleft lip. The application of this technology to the analysis of facial form in this population is evolving. Traditional anthropometric measurements have been used to compare subjects with clefts to subjects without clefts (Weinberg et al., 2009; Hoefert et al., 2010; Bugaighis et al., 2014; Othman et al., 2014), to assess symmetry following cleft lip repair (Nkenke et al., 2006; Stauber et al., 2008; Bugaighis et al., 2014), and to document changes in nasolabial form before and after surgery (Hood et al., 2003; Schwenzler-Zimmerer et al., 2008; Van Loon, et al., 2010; Tse et al., 2015). This relies upon accurate placement of landmarks on a 3D image, which is tedious and can be impractical. Although computer vision methods that can automatically generate landmarks on 3D facial images have been developed (Perakis et al., 2010, 2013; Liang et al., 2013), their accuracy in subjects with clefts is limited. The landmarks generated near cleft regions can be inaccurate and cannot be used for direct measurement. In addition, the landmark-based

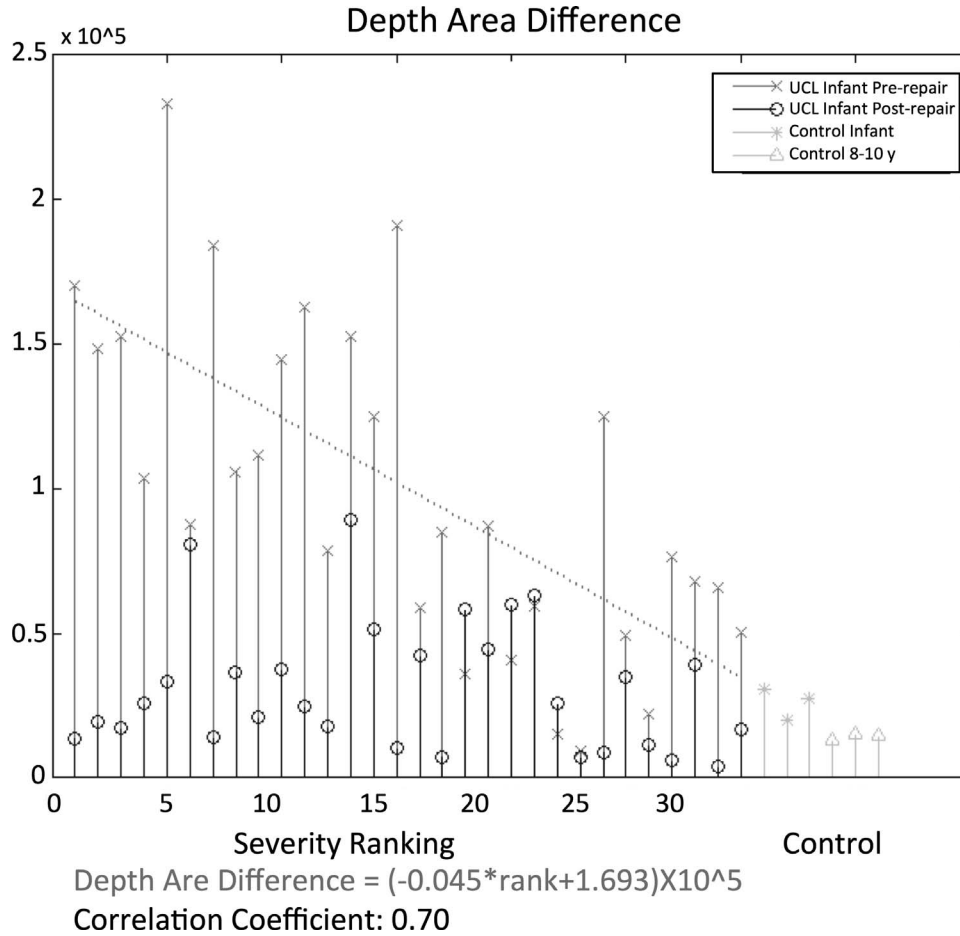


**FIGURE 4** Nasal symmetry: Depth Area Difference. Infant subjects with UCL were ranked in descending order of severity of preoperative cleft lip nasal deformity (by an expert cleft surgeon). For each subject with UCL, the preoperative Depth Area Difference is represented in red (x), and the postoperative Depth Area Difference is represented in blue (o). Preoperative measures converged with postoperative measures and normalized to a level similar to that of the control subjects (green). Preoperative Depth Area Difference correlated well with initial severity of nasal deformity.

measurements use only small numbers of sparse 3D points and fail to take the advantage of other information on the dense face meshes.

Only a few studies have reported the use of non-landmark-based analysis of facial form. The localized facial asymmetry in subjects with clefts to the midface (Meyer-Marcotty et al., 2010; Djordjevic et al., 2014). Nakamura et al. (2010) used color maps to illustrate changes with secondary nasal surgery and Proff et al. (2016) have examined contours along sectional planes. Van Loon et al. (2010) used nasal surface data to quantify asymmetry in older children with previous cleft lip repair; however, this analysis required manual surface landmarking. We have developed a system of analysis that is objective, automated, and requires no manual landmarks.

We used previously described methods that automatically precleaned all the 3D meshes (face recognized and all other body parts are removed) and aligned them to a standard frontal pose using our previous method (Wu et al., 2014). Given that we wanted to focus specifically on the nose rather than on larger regions, we further refined facial

alignment and normalization using the Face++ (Megvii Inc.) software package. This tool accurately identifies a large number of facial landmarks that could be used to refine pose normalization and further define the region of interest. Analysis could then accurately consider all of the available surface data within the specific region.

We used the Depth Area Difference as a measure of nasal symmetry. We used a normative data set and PCA Reconstruction Error as a measure of how “normal” the shape of a nose was. We found that both of these measures could quantify changes through surgery and could differentiate normal control subjects from subjects who have undergone cleft lip repair. In contrast to other reports proposing 3D shape-based analysis (Weinberg et al., 2009; Hoefert et al., 2010; Bugaighis et al., 2014; Othman et al., 2014), we examined content validity by comparing measured values to cleft type and expert ranked preoperative severity for the infant subjects. We found that infants with different types of cleft lip had significantly different measures of nasal symmetry and normalcy and that these corresponded with clinical expectations (i.e., the more

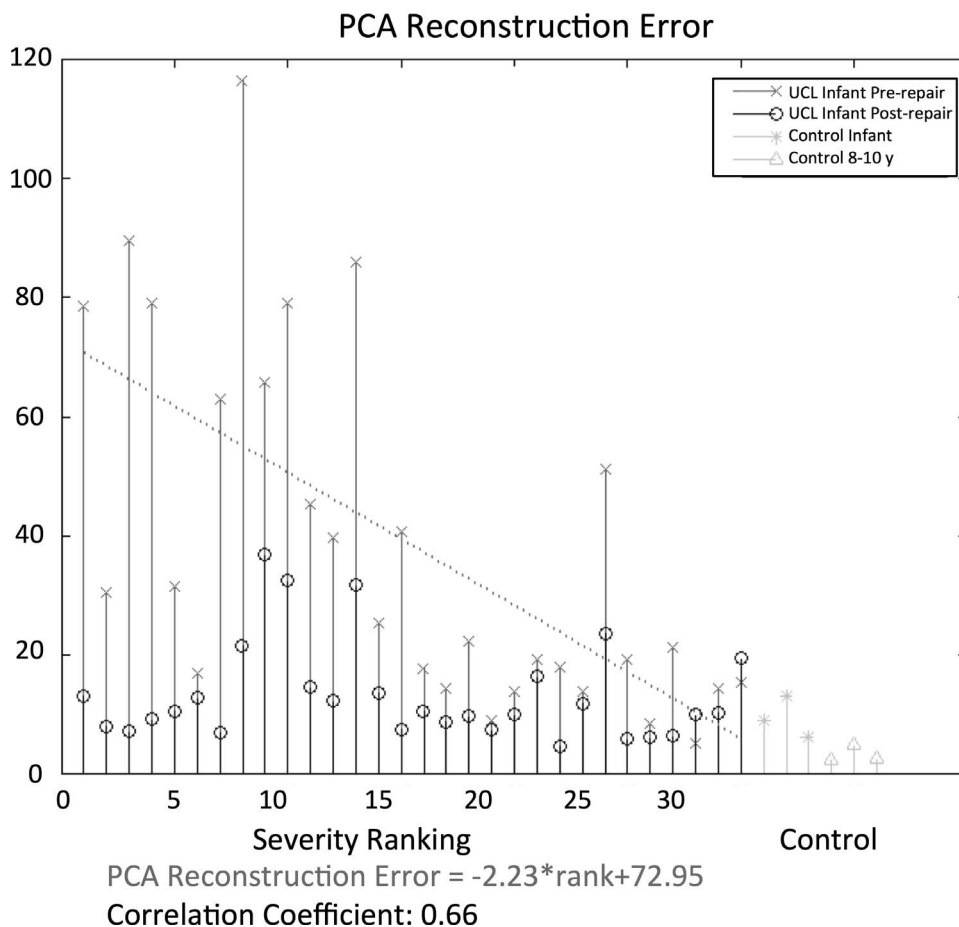


**FIGURE 5 Nasal normalcy: PCA Reconstruction Error.** An expert cleft surgeon ranked infant subjects with UCL in descending order of severity of preoperative cleft lip nasal deformity. The preoperative PCA Reconstruction Error is represented in red (x), and the postoperative PCA Reconstruction Error is represented in blue (o) for each subject with UCL. Preoperative measures converged with postoperative measures and normalized to a similar level to that of the control subjects (green). Preoperative PCA Reconstruction Error had moderate correlation with the initial severity of nasal deformity.

complete the cleft, the greater the measured asymmetry and abnormality). We also found a high correlation for preoperative Depth Area Difference and PCA Reconstruction Error to expert ranked preoperative cleft lip nasal deformity (coefficients of 0.70 and 0.66, respectively). We found that preoperative measures converged with postoperative measures when subjects were arranged in decreasing order of severity, which is consistent with larger improvements in form achieved in more severe cases.

Although there was a lower correlation of PCA Reconstruction Error to expert ranked severity, this measure may be more sensitive in detecting subtle postoperative abnormalities. Using this measure, differences in nasal form were still detected for infants with complete cleft lip, as compared to infant with incomplete cleft lip and to infant controls, even after cleft lip repair.

Our long-term goal is to be able to measure longitudinal changes so that long-term outcomes or changes with growth can be assessed. Therefore, we used a second group of subjects aged 8 to 10 years as part of our sample set. As expected, we found differences between children with clefts and age-matched normal control subjects and found that

measures of symmetry and normalcy were better than those of infants before surgery.

Although analysis of the older postoperative group followed expected trends, we found that measures of symmetry and normalcy were better for infants immediately following surgery. The demographics of the older group included more subjects with complete cleft lip and more subjects with cleft lip and palate. This group also underwent surgery by different surgeons and using different techniques. While we cannot rule out that nasal form may worsen with time and growth, further longitudinal analysis of subjects with matching preoperative and late postoperative images may provide further insights.

While the initial results of this study are promising, there may be several factors that limit the accuracy of this analysis and that result in variations in measurement. First, we observed that the mesh resolution of 3D images for infants was limited compared to that of older children aged 8 to 10 years. This is due to the relatively small size of infant heads in space. We found also found that infants tended to have more facial expressions captured with their images. While improvements in technology may improve image

resolution, we will need to accept the error from facial expression given the variability of an infant's mood on a given day of image capture. Second, our midfacial reference plane was based upon the geometric midline of eye and mouth landmarks. Maxillary growth disturbances, particularly in older children, could lead to subtle but significant orbital and oral commissure asymmetries. We are currently developing methods to automatically identify the tragus. The additional landmark used for the reference plane will improve accuracy in longitudinal analysis. Third, our PCA analysis was based upon a training model for a normative database that contained images of subjects ranging from 3 to 40 years. We used the entire database of over 2000 so that a model nose including a wide range could be used. It is possible that greater accuracy could be achieved when using normative data for PCA analysis that is specific to the age group being examined and that includes greater ethnic diversity. Currently, we do not have a large number of normative infant images available and such age-matched analysis would require more normative data.

## CONCLUSIONS

We have developed automated methods to measure the symmetry and normalcy of a subject's nose before and after a unilateral cleft lip repair using 3D stereo photogrammetry. By measuring Depth Area Difference and PCA Reconstruction Error, we found significant differences before and after surgery and found that these measurements correlated well with the expert-ranked preoperative severity.

*Acknowledgments:* Thanks to Linda Peters for patient recruitment, Laura Stueckle for IRB management, Karina Martinez-Lopez for administrative support, and Jerrie Bishop for budget management.

## REFERENCES

- Bugaighis I, Mattick CR, Tiddeman B, Hobson R. 3D asymmetry of operated children with oral clefts. *Orthod Craniofac Res.* 2014;17:27–37.
- Djordjevic J, Lewis BM, Donaghy CE, Zhurov AI, Knox J, Hunter L, Richmond S. Facial shape and asymmetry in 5-year-old children with repaired unilateral cleft lip and/or palate: an exploratory study using laser scanning. *Eur J Orthod.* 2014;36:497–505.
- Fisher DM. Unilateral cleft lip repair: an anatomical subunit approximation technique. *Plast Reconstr Surg.* 2005;116:61–71.
- Fisher DM, Tse R, Marcus JR. Objective measurements for grading the primary unilateral cleft lip nasal deformity. *Plast Reconstr Surg.* 2008;122:874–880.
- Hoefert CS, Bacher M, Herberts T, Krimmel M, Reinert S, Hoefert S, Göz G. Implementing a superimposition and measurement model for 3D sagittal analysis of therapy-induced changes in facial soft tissue: a pilot study. *J Orofac Orthop/Fortschritte der Kieferorthopädie.* 2010;71:221–234.
- Hood CA, Bock M, Hosey MT, Bowman A, Ayoub AF. Facial asymmetry – 3D assessment of infants with cleft lip & palate. *Int J Paediatr Dent.* 2003;13:404–410.
- Jolliffe I. *Principal Component Analysis.* Wiley Online Library; 2002.
- Liang S, Wu J, Weinberg S M, Shapiro LG. Improved detection of landmarks on 3D human face data. *Conf Proc IEEE Eng Med Biol Soc.* 2013:6482–6485.
- Megvii Inc. Face++ Research Toolkit. Available at www.faceplusplus.com. Accessed March 2015.
- Meyer-Marcotty P, Alpers GW, Gerdes ABM, Stellzig-Eisenhauer A. Impact of facial asymmetry in visual perception: a 3-dimensional data analysis. *Am J Orthod Dentofacial Orthop.* 2010;137:168.e1–8.
- Nakamura N, Okawachi T, Nishihara K, Hirahara N, Nozoe E. Surgical technique for secondary correction of unilateral cleft lip-nose deformity: clinical and 3-dimensional observations of preoperative and postoperative nasal forms. *J Oral Maxillofac Surg.* 2010;68:2248–2257.
- Nkenke E, Lehner B, Kramer M, Haeusler G, Benz S, Schuster M, Neukam FW, Vairaktaris EG, Wum J. Determination of facial symmetry in unilateral cleft lip and palate patients from three-dimensional data: technical report and assessment of measurement errors. *Cleft Palate Craniofac J.* 2006;43:129–137.
- Othman SA, Ahmad R, Asi SM, Ismail NH, Rahman ZAA. Three-dimensional quantitative evaluation of facial morphology in adults with unilateral cleft lip and palate, and patients without clefts. *Br J Oral Maxillofac Surg.* 2014;52:208–213.
- Paker SE, Mai CT, Canfield MA, Rickard R, Wang Y, Meyer RE, Anderson P, Mason CA, Collins JS, Kirby RS, et al; National Birth Defects Prevention Network. Updated national birth prevalence estimates for selected birth defects in the United States, 2004–2006. *Birth Defects Res A Clin Mol Teratol.* 2010;88:1008–1016.
- Perakis P, Passalis G, Theoharis T, Kakadiaris IA. 3D Facial landmark detection & face registration. *IEEE TPAMI.* 2010;35:1552–1564.
- Perakis P, Passalis G, Theoharis T, Kakadiaris IA. 3D facial landmark detection under large yaw and expression variations. *IEEE Trans Pattern Anal Mach Intell.* 2013;35:1552–1564.
- Proff P, Weingaertner J, Rottner K, Bayerlein T, Schoebel S, Kaduk W, Gedrange T. Functional 3-D analysis of patients with unilateral cleft of lip, alveolus and palate (UCLAP) following lip repair. *J Craniomaxillofac Surg.* 2006;34:26–30.
- Schwenzer-Zimmerer K, Chaitidis D, Derg-Boemer I, Krol Z, Kovacs L, Schwenzer NF, Zimmerer S, Holberg C, Zeilhofer HF. Quantitative 3D soft tissue analysis of symmetry prior to and after unilateral cleft lip repair compared with non-cleft persons (performed in Cambodia). *J Craniomaxillofac Surg.* 2008;36:431–438.
- Sirovich L, Kirby M. Low-dimensional procedure for the characterization of human faces. *J Opt Soc Am A.* 1987;4:519–524.
- Stauber I, Vairaktaris E, Holst A, Schuster M, Hirschfelder U, Neukam F, Nkenke E. Three-dimensional analysis of facial symmetry in cleft lip and palate patients using optical surface data. *J Orofac Orthop.* 2008; 694:268–282.
- Tse R. Unilateral cleft lip: principles and practice of surgical management. *Semin Plast Surg.* 2013;26:145–155.
- Tse R, Lien S. Unilateral cleft lip repair using the “anatomic subunit approximation”: modifications and analysis of early results in 100 consecutive cases. *Plast Reconstr Surg.* 2015;136:119–130.
- Van Loon B, Maal TJ, Plooi JM, Ingels KJ, Borstlap WA, Kuijpers-Jagtman AM, Spauwen PH, Berge SJ. 3D stereophotogrammetric assessment of pre-and postoperative volumetric changes in the cleft lip and palate nose. *Int J Oral Maxillofac Surg.* 2010;39:534–540.
- Weinberg SM, Naidoo SD, Bardi KM, Brandon CA, Neiswanger K, Resick JM, Martin RA, Marazita ML. Face shape of unaffected parents with cleft affected offspring: combining three-dimensional

- surface imaging and geometric morphometrics. *Orthod Craniofac Res.* 2009;12 271–281.
- Wu J, Heike C, Birgfeld C, Evans K, Maga M, Morrison C, Saltzman B, Shapiro L, Tse R. Measuring symmetry in children with unrepaired cleft lip: defining a standard for the 3D mid-facial reference plane. *Cleft Palate Craniofac J.* In press.
- Wu J, Liang S, Shapiro L, Tse R. Measuring symmetry in children with cleft lip. Part 2: Quantification of nasolabial symmetry before and after cleft repair. *Cleft Palate Craniofacial Journal.* In press.
- Wu J, Tse R, Shapiro L. Automated face extraction and normalization of 3D Mesh Data. *Conf Proc IEEE Eng Med Biol Soc.* 2014;750–753.